



Turn-On Luminescent Probes for the Real-Time Monitoring of Endogenous Hydroxyl Radicals in Living Cells

Wenjuan Zhou, Yuqing Cao, Dandan Sui, and Chao Lu*

Abstract: The utilization of semiconductor quantum dots (QDs) as optical labels for biosensing and biorecognition has made substantial progress. However, the development of a suitable QD-based luminescent probe that is capable of detecting individual reactive oxygen species (ROS) represents a great challenge, mainly because the fluorescence of QDs is quenched by a wide variety of ROS. To overcome this limitation, a novel QD-based turn-on luminescent probe for the specific detection of $\cdot\text{OH}$ has been designed, and its application in monitoring the endogenous release of $\cdot\text{OH}$ species in living cells is demonstrated. Metal citrate complexes on the surfaces of the QDs can act as electron donors, injecting electrons into the LUMO of the QDs, while $\cdot\text{OH}$ can inject holes into the HOMO of the QDs. Accordingly, electron-hole pairs are produced, which could emit strong luminescence by electron-hole recombination. Importantly, this luminescent probe does not respond to other ROS.

Reactive oxygen species (ROS) have attracted more and more interest in a variety of fields because of their key roles in physiological and pathological events.^[1] Therefore, monitoring ROS contributes to a better understanding of their biological roles. Currently, fluorescent probes are generally used for the detection of intracellular ROS.^[2] In particular, organic fluorescent probes have been designed for the detection of individual ROS.^[3] However, their applications are limited by their susceptibility to photobleaching, biotoxicity, and spontaneous autoxidation.^[4] Meanwhile, surface-enhanced Raman scattering (SERS) has been successfully developed as a promising alternative to fluorescence measurements that benefits from the photostability and narrow spectral band of the used probes.^[5]

Several new strategies for the synthesis of functionalized semiconductor quantum dots (QDs) with substrate-specific ligands or receptor units have been implemented to develop optical sensing systems for a variety of cellular imaging methods and the detection of chemicals and biomolecules.^[6] However, a wide variety of ROS can quench the fluorescence of QDs,^[7] impeding the practical application of QDs as a fluorescent probe for an individual ROS. Therefore, to elucidate potential pathophysiological processes associated with the target ROS, the development of a suitable QD-based

luminescent probe that is capable of detecting individual ROS is crucial.

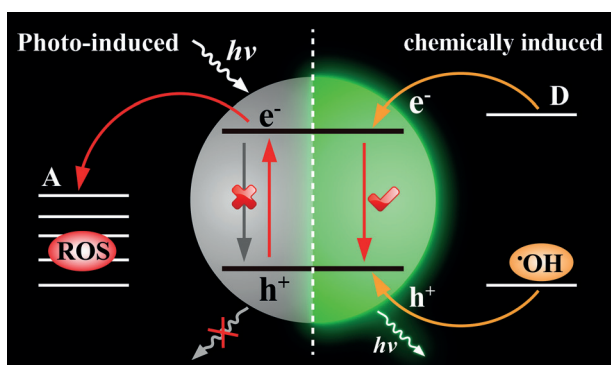
Photoexcitation of valence-band electrons into the conduction band of QDs yields electron-hole pairs that recombine to generate photoluminescence. However, two competitive electron-transfer routes, namely by electron-acceptor or electron-donor units, can prevent the recombination of the electron-hole pairs on the photoexcited QDs, quenching the fluorescence of the QDs.^[6c] Alternatively, the luminescence of QDs can be recovered by the following process: The injection of an electron from an electron-donor unit into the LUMO of a QD produces a reducing QD (QD^-), and the injection of a hole from an electron acceptor into the HOMO of a QD generates an oxidizing QD (QD^+);^[8] the recombination of QD^- and QD^+ results in the formation of excited-state QDs, which can generate strong luminescence by electron-transfer recombination.^[8b] Interestingly, only $\cdot\text{OH}$ can easily inject a hole into the 1S_h quantum-confined orbital of the QD core as the $\cdot\text{OH}/\text{OH}^-$ couple displays the highest standard redox potential of all ROS.^[9] Inspired by this property of $\cdot\text{OH}$, we were interested in developing a specific QD-based luminescent probe for $\cdot\text{OH}$ detection by making use of electron donors with matching energy levels.

Citrate is an excellent candidate to substitute thiol capping ligands in the synthesis of water-soluble QDs owing to its low toxicity and good biocompatibility.^[10] On the other hand, citrate can act as an electron donor on a metal surface.^[11] Taking into account these impressive properties, we anticipated that citrate should be an ideal electron donor. We herein report that a metal citrate complex on the surface of a CdTe QD can inject electrons into the LUMO of the CdTe QD core. In combination with the hole injection from $\cdot\text{OH}$, excited-state QDs will be formed, which can emit light when returning to the ground state (Scheme 1). This luminescent probe is capable of detecting $\cdot\text{OH}$ with high selectivity, and the overall approach was validated by monitoring the endogenous release of $\cdot\text{OH}$ in living cells. The proposed strategy has great potential for studying pathophysiological processes associated with $\cdot\text{OH}$ species by selectively and sensitively monitoring intracellular $\cdot\text{OH}$ levels.

Citrate-capped CdTe QDs (Figure 1A; see also the Supporting Information, Figure S1) were synthesized by mixing thioglycolic acid (TGA) capped CdTe QDs (Figure S2) with fluorosurfactant-capped gold nanoparticles (FSN-AuNPs).^[12] A UV/Vis absorption spectrum and a TEM image of the FSN-AuNPs (14 nm) are shown in Figure S3A. Thiol-induced aggregation of the AuNPs was observed upon ligand exchange (Figure S3B). These AuNP aggregates could be easily separated from the CdTe QDs by

[*] Dr. W. J. Zhou, Y. Q. Cao, Dr. D. D. Sui, Prof. Dr. C. Lu
State Key Laboratory of Chemical Resource Engineering
Beijing University of Chemical Technology
PO Box 79, 100029, Beijing (China)
E-mail: luchao@mail.buct.edu.cn

Supporting information for this article can be found under <http://dx.doi.org/10.1002/anie.201511868>.



Scheme 1. Photoluminescence quenching of QDs by ROS electron acceptors (A) and chemical-reaction-induced luminescence of QDs by electron-hole recombination in the QDs in the presence of metal citrate complexes as electron donors (D) and ·OH species as hole donors.

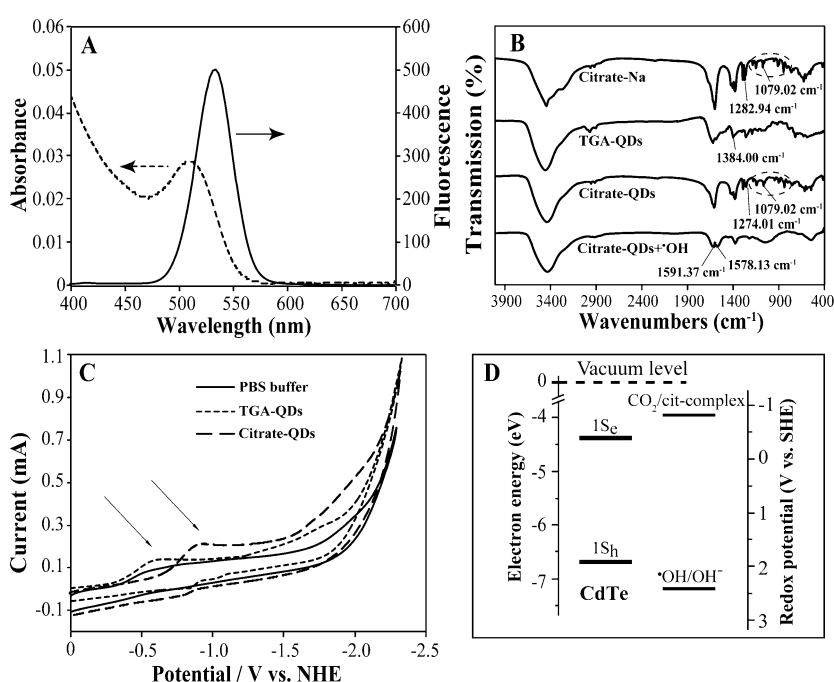


Figure 1. A) Fluorescence ($\lambda_{\text{ex}} = 365$ nm, ex/em slits: 5.0 nm) and UV/Vis absorption spectra of the citrate-capped CdTe QDs. B) FT-IR spectra of sodium citrate (citrate-Na), TGA-capped CdTe QDs (TGA-QDs), and citrate-capped CdTe QDs (citrate-QDs), and of the reaction products of citrate-capped CdTe QDs with ·OH. C) Cyclic voltammograms recorded for PBS buffer (50 mM, pH 7.4), TGA-QDs (PBS, pH 7.4), and citrate-QDs (PBS, pH 7.4). Scan rate: 100 mV s⁻¹; working electrode: glassy carbon electrode; reference electrode: Ag/AgCl electrode; counter electrode: Pt electrode. D) Energy level diagram for the 1S_h and 1S_e quantum-confined orbitals of the CdTe QDs, and the standard redox potentials of ·OH and the QD citrate complex (cit-complex).

centrifugation. The success of ligand exchange was confirmed by Fourier transform infrared (FT-IR) spectroscopy (Figure 1B). The absorption band at 1283 cm⁻¹, which corresponds to the C–O stretching vibrations, was shifted towards lower frequencies (1274 cm⁻¹) with a decrease in the intensity (Figure 1B), demonstrating the bonding of citrate to the CdTe QDs through the C–O groups.^[10b,13] Furthermore, energy-dispersive X-ray spectroscopy (EDX) data demonstrated the

complete removal of the thiol ligands from the surface of the CdTe QDs after ligand exchange (Figure S4).

The changes in the energy levels of the CdTe QDs were monitored by cyclic voltammetry. For the TGA-capped CdTe QDs, a cathodic peak was observed at approximately −0.65 V (Figure 1C), which was attributed to the formation of the stable radical anion of the CdTe QDs.^[14] The LUMO energy level of the CdTe QDs was calculated to be −4.41 eV, according to the equation $E_{\text{LUMO}} = -(E_{\text{onset}}^{\text{red}} + 4.71)$ eV,^[15] where the onset reduction potential ($E_{\text{onset}}^{\text{red}}$) was determined to be −0.30 V. The HOMO energy level of the CdTe QDs was estimated to be −6.65 eV according to $E_{\text{HOMO}} = E_{\text{LUMO}} - E_{\text{g}}$, where E_{g} is the optical band gap ($E_{\text{g}} = 1240/\lambda_{\text{g}}$, where λ_{g} is absorption edge of the CdTe QDs).^[16] For the citrate-capped CdTe QDs, a well-defined cathodic peak was observed at −0.96 V (Figure 1C), indicating the formation of metal citrate complexes on the surface of the QDs.^[17] Accordingly, because of the more cathodic value, the complex shell can inject electrons into the LUMO of the CdTe QD core (Figure 1D).

In general, electron transfer from the conduction band of the QDs to the singly occupied molecular orbitals of ROS could lead to the fluorescence quenching of the QDs.^[7] In this work, indiscriminate fluorescence quenching was also observed from the citrate-capped CdTe QDs in the presence of a wide variety of ROS (Figure 2A, inset), which implies that it is difficult to differentiate between individual ROS by fluorescence identification with the citrate-capped CdTe QDs. Notably, among various ROS, ·OH shows the most positive redox potential ($\cdot\text{OH} + \text{e}^- \rightarrow \text{OH}^-$, $E_0 \approx (2.84 - 0.06 \text{ pH})$ V vs. SHE), which is sufficient for hole injection into the 1S_h quantum-confined orbital of the CdTe core to produce QD⁺ (Figure 1D).^[8b] In combination with the injection of electrons into the LUMO of the QD core by the citrate complex shell, excited-state QDs will be formed. Accordingly, a strong luminescence signal was detected with the static injection setup shown in Figure S5. However, no obvious emission could be initiated by other ROS, including ¹O₂, H₂O₂, O₂^{·-}, ClO⁻, TBHP, TBO[·], and ROO[·] (Figure 2A), indicating the good selectivity of the QD-based luminescent probe towards ·OH, which is due to the citrate complex on the QD surface. The relatively weak luminescence of the citrate-capped CdTe QDs in the presence of ONOO⁻ arises from a small number of ·OH radicals that are generated by homolysis of ONOOH under physiological conditions.^[18]

The origin of the ·OH-triggered luminescence of the citrate-capped CdTe QDs was investigated in detail. As shown in Figure S6, the luminescence of the citrate-capped CdTe QDs was very strong in the presence of ·OH species. However, very weak emission was observed with the TGA-

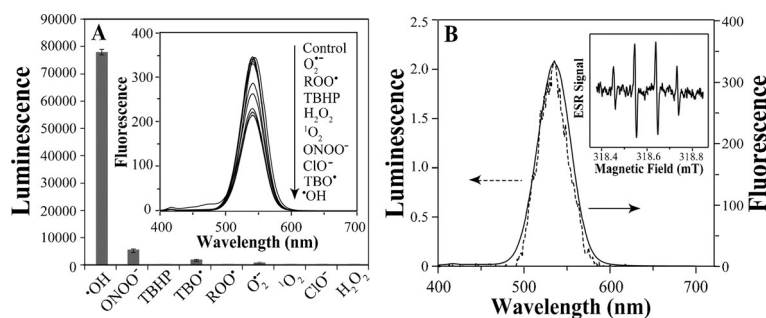


Figure 2. A) Luminescence intensity of the citrate-capped CdTe QDs in the presence of different ROS. Inset: Fluorescence spectra of the citrate-capped CdTe QDs after the addition of different ROS. B) Fluorescence spectrum of the citrate-capped QDs (solid line) and luminescence spectrum of the citrate-capped CdTe QD/[•]OH system (dotted line). Inset: ESR signal of the DMPO-[•]OH adduct in the citrate-capped CdTe QD/[•]OH system. All experiments were performed at room temperature in 50 mM PBS buffer (pH 7.4). The concentration of the citrate-capped CdTe QDs was 0.4 μ M, and the concentration of the ROS was 100 μ M. Fluorescence spectra were monitored using $\lambda_{\text{ex}} = 365$ nm. The luminescence spectrum was obtained with a fluorescence spectrophotometer without excitation light.

capped CdTe QDs and in other control experiments. These results indicate that the citrate complex on the surface of the CdTe QDs makes a decisive contribution to the strong emission in the citrate-capped CdTe QD/[•]OH system. Furthermore, the evolution of the citrate consumption during the reaction was monitored by FT-IR spectroscopy (Figure 1B). After the addition of [•]OH, the FT-IR spectrum of the citrate-capped CdTe QDs shows a new band at 1578 cm^{-1} , which corresponds to asymmetric C=O stretching vibrations of the ketone groups.^[19] These results demonstrate that the metal citrate complexes on the surfaces of the CdTe QDs can donate electrons and decompose into acetonedicarboxylate in the presence of [•]OH.^[11] The nature of the emitting species in the citrate-capped CdTe QD/[•]OH system was confirmed by measuring the luminescence spectrum. Maximum emission was observed at $\lambda \approx 535$ nm (Figure 2B), which is consistent with the fluorescence spectrum of the citrate-capped CdTe QDs. The overlapping nature of the spectra confirms that the reaction between the citrate-capped CdTe QDs and [•]OH can generate excited-state CdTe QDs.^[8c] Furthermore, the reactive intermediates of the citrate-capped CdTe QD/[•]OH system were also analyzed by electron spin resonance (ESR) spectroscopy and the addition of ROS scavengers. For the ESR experiments, 5,5-dimethyl-1-pyrroline *N*-oxide (DMPO) was used as a specific target molecule of [•]OH. A significant ESR signal corresponding to the DMPO-[•]OH adduct was observed (Figure 2B, inset), indicating the presence of [•]OH in the proposed system. Moreover, the luminescence intensity of the system was remarkably quenched when [•]OH scavengers (thiourea, DMSO, and *t*BuOH)^[20] were added (Figure S7). On the other hand, these scavengers had no effect on the luminescence properties of the citrate-capped CdTe QDs. These results further demonstrate that the strong emission of the proposed system is due to the presence of [•]OH.

Having shown the superior analytical performance of the citrate-capped CdTe QDs for monitoring [•]OH in vitro, such as

excellent linearity, stable read-out, and reversible sensing (Figures S8 and S9), we then explored its capability as a turn-on luminescent probe for intracellular [•]OH assays. First, the toxicity of the citrate-capped CdTe QDs towards HeLa cells was evaluated according to the MTT viability assay. The results indicated that the HeLa cells maintained a high viability (> 80 %) after they had been incubated with the citrate-capped CdTe QDs (0.1 μ M) for twelve hours (Figure S10). Therefore, the citrate-capped CdTe QDs could be used as intracellular luminescent probes. On the other hand, the cellular uptake of the as-proposed probe was investigated by incubating cells with the citrate-capped CdTe QDs at various concentrations for four hours. The uptake first increased with an increase in the concentration of the citrate-capped CdTe QDs and reached a saturation point in the presence of 0.1 μ M citrate-capped CdTe QDs (Figure S11).

Generally, nanoparticles undergo endocytosis through the endosomal pathway, and are eventually transferred to the lysosomes.^[21] The intracellular localization of the citrate-capped CdTe QDs was determined by co-staining with organelle markers.^[22] Figures 3A and B show that the CdTe QDs internalized by HeLa cells were primarily localized within the lysosomes. We then investigated the stability of the citrate-capped CdTe QDs against five proteases (trypsin, pronase, proteinase 3, proteinase K, and cathepsin G).^[23] No fluorescence quenching of the citrate-capped CdTe QDs was observed upon incubation with these proteases for six hours at 37 °C (Figure S12). The fluorescence enhancement observed in the presence of trypsin might be due to the adsorption of the protein on the surface of the QDs.^[24] On the other hand, there was almost no change in the luminescence response of the citrate-capped CdTe QDs towards [•]OH in the presence of the five tested proteases. Therefore, we concluded that the citrate ligand shells on the surfaces of the CdTe QDs were not destructed by the proteases.

The Fenton reaction ($\text{Fe}^{2+}/\text{H}_2\text{O}_2$) was used to produce exogenous [•]OH in living cells.^[25] After incubation with 0.1 μ M citrate-capped CdTe QDs (Figure 3A and B), the cells were treated with a series of H_2O_2 concentrations. Then the luminescence signals were recorded when 1.0 mM Fe^{2+} solutions were injected into the cells. The relative luminescence intensity was approximately linearly dependent on the [•]OH concentration within the cells (Figure 3C). The calibration curve was found to be linear from 0.1 to 100 μ M with a regression line of $y = 10x + 26.767$ ($R^2 = 0.9995$), where y is the luminescence intensity, and x is the [•]OH concentration. The relative standard deviation for nine repeated measurements with 1.0 μ M H_2O_2 was 2.8 %.

To confirm that the proposed luminescent probe is specific to [•]OH, we performed a control experiment by treating QD-loaded cells with 100 μ M H_2O_2 and 0.1 % DMSO for 30 min.^[20c] Interestingly, a clear inhibitory effect of DMSO on the luminescence intensity was observed after injecting 1.0 mM Fe^{2+} (Figure 3D), further confirming that the lumi-

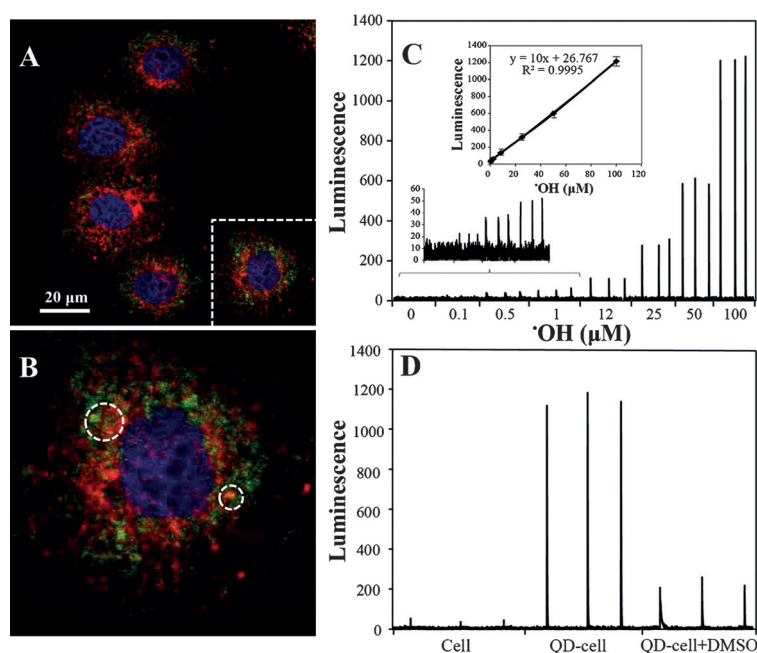


Figure 3. A) Intracellular localization of the citrate-capped CdTe QDs in stained HeLa cells (QDs: green; lysosomes: red; nucleus: blue). B) Magnified image of the indicated region in (A). C) Luminescence response of cells loaded with the citrate-capped CdTe QDs towards different $\cdot\text{OH}$ concentrations. Inset: Calibration curve for $\cdot\text{OH}$. D) Luminescence response of the HeLa cells, cells loaded with the citrate-capped CdTe QDs, and cells loaded with the citrate-capped CdTe QDs and treated with 0.1% DMSO towards 100 μM $\cdot\text{OH}$.

nescence of the proposed probe is due to the presence of $\cdot\text{OH}$ in the living cells. Finally, the effects of some typical interfering compounds (e.g., some ions and reductants) in living cells were investigated. Fortunately, these substances had no influence on the detection of 10 μM $\cdot\text{OH}$ (Table S1). It is known that glutathione (in the mM range) is the most important antioxidant in living cells counteracting the deleterious effects of oxidative stress.^[26] Herein, we investigated the effect of glutathione on the luminescence of the citrate-capped CdTe QD/ $\cdot\text{OH}$ system in detail. As shown in Figure S13, $\cdot\text{OH}$ was partially scavenged by glutathione in the range of 2.0–10 mM. Therefore, the proposed luminescent probe can monitor the net release of ROS in the stimulation process.

The ability of the proposed probe to monitor $\cdot\text{OH}$ generated upon physiological stimulation was examined by using phorbol 12-myristate 13-acetate (PMA) to stimulate the endogenous production of ROS in living cells.^[27] In this assay, HeLa cells were first incubated with the citrate-capped CdTe QDs for four hours, followed by luminescence measurements before/after PMA stimulation (Figure 4A). The luminescence signal increased gradually after PMA stimulation and reached its maximum within 1.5 hours (Figure 4B). However, the luminescence signal decreased to the control level after four hours of stimulation, indicating that the PMA-induced $\cdot\text{OH}$ release was completed in four hours. Note that stable luminescence signals were recorded for more than one hour before stimulation. Furthermore, the real-time monitoring was repeated, and thus has some biological meaning (Fig-

ure S14). Citrate-capped CdTe QDs in HeLa cells were still observed to fluoresce after four hours of PMA stimulation (Figure 4C and D), confirming that the content of citrate-capped CdTe QDs in the HeLa cells was enough for measuring the released $\cdot\text{OH}$ under PMA stimulation. Therefore, the proposed luminescent probe can be used for the real-time monitoring of $\cdot\text{OH}$ production in living cells.

In summary, we have developed a highly selective turn-on luminescent probe for $\cdot\text{OH}$ species that makes use of metal citrate complexes on the surface of CdTe QDs. These complexes inject electrons into the LUMO of the CdTe QDs while the $\cdot\text{OH}$ species act as electron acceptors, injecting holes into the HOMO of the CdTe QDs. Other types of fluorescent probes for $\cdot\text{OH}$ are mainly based on small organic molecules and nanoparticles. The probes obtained from small organic molecules exhibit high sensitivity and specificity with regard to $\cdot\text{OH}$ detection whereas the sensitivity and specificity of some nanoparticle probes towards $\cdot\text{OH}$ are unsatisfactory. Our QD-based probe for the detection of $\cdot\text{OH}$ benefits from a facile preparation method and high selectivity and sensitivity (Table S2). Studies with living cells revealed that the citrate-capped CdTe QDs display a specific response towards $\cdot\text{OH}$ and excellent optical properties, low cytotoxicity,

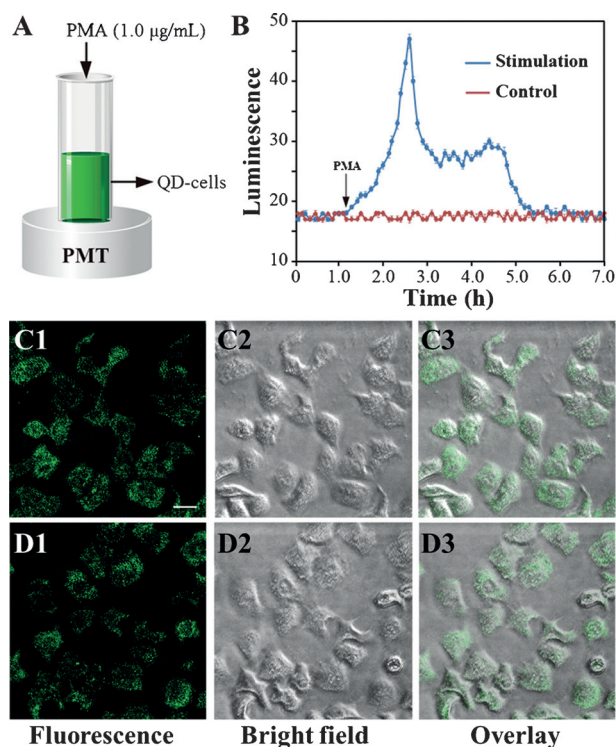


Figure 4. A) Real-time detection of generated $\cdot\text{OH}$ species by PMA in living cells. B) Real-time luminescence response of $\cdot\text{OH}$ species generated by 1.0 μg mL⁻¹ PMA stimulation in living cells. C, D) Confocal fluorescence microscopy images of HeLa cells incubated with 0.1 μM citrate-capped CdTe QDs for 4 h (C) that were then treated with 1.0 μg mL⁻¹ PMA for 4 h (D). Scale bar: 40 μm.

and good biocompatibility. The proposed system has been successfully applied for the real-time monitoring of $\cdot\text{OH}$ generated in living cells under PMA stimulation. This method will expand the applicability of QDs as biosensors, helping to unravel the role of endogenous ROS in complicated biological systems.

Acknowledgements

This work was supported by the National Basic Research Program of China (973 Program, 2014CB932103), the National Natural Science Foundation of China (21575010 and 21375006), and the Innovation and Promotion Project of the Beijing University of Chemical Technology. We thank Prof. B. Z. Tang (The Hong Kong University of Science & Technology) for his advice on data analysis.

Keywords: hydroxyl radicals · living cells · luminescent probes · quantum dots · real-time monitoring

How to cite: *Angew. Chem. Int. Ed.* **2016**, *55*, 4236–4241
Angew. Chem. **2016**, *128*, 4308–4313

- [1] a) T. Finkel, N. J. Holbrook, *Nature* **2000**, *408*, 239–247; b) B. C. Dickinson, C. J. Chang, *Nat. Chem. Biol.* **2011**, *7*, 504–511; c) T. T. Chen, Y. Hu, Y. Cen, X. Chu, Y. Lu, *J. Am. Chem. Soc.* **2013**, *135*, 11595–11602; d) R. Kojima, H. Takakura, M. Kamiya, E. Kobayashi, T. Komatsu, T. Ueno, T. Terai, K. Hanaoka, T. Nagano, Y. Urano, *Angew. Chem. Int. Ed.* **2015**, *54*, 14768–14771; *Angew. Chem.* **2015**, *127*, 14981–14984; e) H.-S. Wang, W.-J. Bao, S.-B. Ren, M. Chen, K. Wang, X.-H. Xia, *Anal. Chem.* **2015**, *87*, 6828–6833.
- [2] a) X. Q. Chen, X. Z. Tian, I. Shin, J. Yoon, *Chem. Soc. Rev.* **2011**, *40*, 4783–4804; b) Y. Koide, Y. Urano, S. Kenmoku, H. Kojima, T. Nagano, *J. Am. Chem. Soc.* **2007**, *129*, 10324–10325; c) Y. Koide, M. Kawaguchi, Y. Urano, K. Hanaoka, T. Komatsu, M. Abo, T. Terai, T. Nagano, *Chem. Commun.* **2012**, *48*, 3091–3093.
- [3] a) B. C. Dickinson, C. Huynh, C. J. Chang, *J. Am. Chem. Soc.* **2010**, *132*, 5906–5915; b) W. Zhang, W. Liu, P. Li, F. Huang, H. Wang, B. Tang, *Anal. Chem.* **2015**, *87*, 9825–9828; c) Q. L. Xu, K. A. Lee, S. Lee, K. M. Lee, W. J. Lee, J. Yoon, *J. Am. Chem. Soc.* **2013**, *135*, 9944–9949; d) L. Yuan, L. Wang, B. K. Agrawalla, S. J. Park, H. Zhu, B. Sivaraman, J. Peng, Q. H. Xu, Y. T. Chang, *J. Am. Chem. Soc.* **2015**, *137*, 5930–5938; e) T. Peng, N. K. Wong, X. M. Chen, Y. K. Chan, D. H. Ho, Z. N. Sun, J. J. Hu, J. G. Shen, H. El-Nezami, D. Yang, *J. Am. Chem. Soc.* **2014**, *136*, 11728–11734; f) J. J. Hu, N. K. Wong, S. Ye, X. M. Chen, M.-Y. Lu, A. Q. Zhao, Y. H. Guo, A. C. Ma, A. Y. Leung, J. G. Shen, D. Yang, *J. Am. Chem. Soc.* **2015**, *137*, 6837–6843.
- [4] a) H. Kobayashi, M. Ogawa, R. Alford, P. L. Choyke, Y. Urano, *Chem. Rev.* **2010**, *110*, 2620–2640; b) Y. Koide, Y. Urano, K. Hanaoka, T. Terai, T. Nagano, *J. Am. Chem. Soc.* **2011**, *133*, 5680–5682; c) Q. Q. Wan, S. M. Chen, W. Shi, L. H. Li, H. M. Ma, *Angew. Chem. Int. Ed.* **2014**, *53*, 10916–10920; *Angew. Chem.* **2014**, *126*, 11096–11100.
- [5] a) S. Keren, C. Zavaleta, Z. Cheng, A. de la Zerda, O. Gheysens, S. S. Gambhir, *Proc. Natl. Acad. Sci. USA* **2008**, *105*, 5844–5849; b) E. S. Allgeyer, A. Pongan, M. Browne, M. D. Mason, *Nano Lett.* **2009**, *9*, 3816–3819; c) P. Rivera-Gil, C. Vazquez-Vazquez, V. Giannini, M. P. Callao, W. J. Parak, M. A. Correa-Duarte, R. A. Alvarez-Puebla, *Angew. Chem. Int. Ed.* **2013**, *52*, 13694–13698; *Angew. Chem.* **2013**, *125*, 13939–13943.
- [6] a) X. Michalet, F. F. Pinaud, L. A. Bentolila, J. M. Tsay, S. Doose, J. J. Li, G. Sundaresan, A. M. Wu, S. S. Gambhir, S. Weiss, *Science* **2005**, *307*, 538–544; b) R. Gill, M. Zayats, I. Willner, *Angew. Chem. Int. Ed.* **2008**, *47*, 7602–7625; *Angew. Chem.* **2008**, *120*, 7714–7736; c) R. Freeman, I. Willner, *Chem. Soc. Rev.* **2012**, *41*, 4067–4085; d) J. Zhou, Y. Yang, C.-Y. Zhang, *Chem. Rev.* **2015**, *115*, 11669–11717; e) K. D. Wegner, N. Hildebrandt, *Chem. Soc. Rev.* **2015**, *44*, 4792–4834; f) A. S. Susa, A. M. Javier, W. J. Parak, A. L. Rogach, *Colloids Surf. A* **2006**, *281*, 40–43.
- [7] a) Z. P. Wang, J. Li, B. Liu, J. Q. Hu, X. Yao, J. H. Li, *J. Phys. Chem. B* **2005**, *109*, 23304–23311; b) H. Chen, L. Lin, Z. Lin, G. S. Guo, J.-M. Lin, *J. Phys. Chem. A* **2010**, *114*, 10049–10058; c) K. X. Hay, V. Y. Waisundara, Y. Zong, M.-Y. Han, D. J. Huang, *Small* **2007**, *3*, 290–293.
- [8] a) Z. F. Ding, B. M. Quinn, S. K. Haram, L. E. Pell, B. A. Korgel, A. J. Bard, *Science* **2002**, *296*, 1293–1297; b) S. K. Poznyak, D. V. Talapin, E. V. Shevchenko, H. Weller, *Nano Lett.* **2004**, *4*, 693–698; c) P. Wu, X. D. Hou, J.-J. Xu, H.-Y. Chen, *Chem. Rev.* **2014**, *114*, 11027–11059; d) L. Y. Zheng, Y. W. Chi, Y. Q. Dong, J. P. Lin, B. B. Wang, *J. Am. Chem. Soc.* **2009**, *131*, 4564–4565; e) S. L. Yang, J. S. Liang, S. L. Luo, C. B. Liu, Y. H. Tang, *Anal. Chem.* **2013**, *85*, 7720–7725.
- [9] H. Chen, L. Lin, H. F. Li, J.-M. Lin, *Coord. Chem. Rev.* **2014**, *263*–264, 86–100.
- [10] a) P. P. Ingole, R. M. Abhyankar, B. L. V. Prasad, S. K. Haram, *Mater. Sci. Eng. B* **2010**, *168*, 60–65; b) M. Hu, H. L. Yu, F. D. Wei, G. H. Xu, J. Yang, Z. Cai, Q. Hu, *Spectrochim. Acta Part A* **2012**, *91*, 130–135.
- [11] a) X. M. Wu, P. L. Redmond, H. T. Liu, Y. H. Chen, M. Steigerwald, L. E. Brus, *J. Am. Chem. Soc.* **2008**, *130*, 9500–9506; b) C. Xue, G. S. Metraux, J. E. Millstone, C. A. Mirkin, *J. Am. Chem. Soc.* **2008**, *130*, 8337–8344; c) E. S. Thrall, A. Preska Steinberg, X. M. Wu, L. E. Brus, *J. Phys. Chem. C* **2013**, *117*, 26238–26247; d) S. Patra, A. K. Pandey, D. Sen, S. V. Ramagiri, J. R. Bellare, S. Mazumder, A. Goswami, *Langmuir* **2014**, *30*, 2460–2469.
- [12] L. Y. Wang, H. X. Zhang, C. Lu, L. X. Zhao, *J. Colloid Interface Sci.* **2014**, *413*, 140–146.
- [13] O. Gylene, J. Aikaite, O. Nivinskiene, *J. Hazard. Mater.* **2004**, *109*, 105–111.
- [14] S. K. Haram, A. Kshirsagar, Y. D. Gujarathi, P. P. Ingole, O. A. Nene, G. B. Markad, S. P. Nanavati, *J. Phys. Chem. C* **2011**, *115*, 6243–6249.
- [15] a) X. M. Liu, H. Xia, W. Gao, Q. L. Wu, X. Fan, Y. Mu, C. S. Ma, *J. Mater. Chem.* **2012**, *22*, 3485–3492; b) K.-T. Lee, C.-H. Lin, S.-Y. Lu, *J. Phys. Chem. C* **2014**, *118*, 14457–14463.
- [16] J. Q. Yu, A. Kudo, *Adv. Funct. Mater.* **2006**, *16*, 2163–2169.
- [17] a) S. M. Pawar, B. S. Pawar, A. V. Moholkar, D. S. Choi, J. H. Yun, J. H. Moon, S. S. Kolekar, J. H. Kim, *Electrochim. Acta* **2010**, *55*, 4057–4061; b) Y. Q. Lai, F. Y. Liu, Z. A. Zhang, J. Liu, Y. Li, S. S. Kuang, J. Li, Y. X. Liu, *Electrochim. Acta* **2009**, *54*, 3004–3010.
- [18] S. Goldstein, J. Lind, G. Merenyi, *Chem. Rev.* **2005**, *105*, 2457–2470.
- [19] R. Castarlenas, M. A. Esteruelas, M. Martin, L. A. Oro, *J. Organomet. Chem.* **1998**, *564*, 241–247.
- [20] a) Z. H. Wang, X. Teng, C. Lu, *Anal. Chem.* **2015**, *87*, 3412–3418; b) H. Chen, H. F. Li, J.-M. Lin, *Anal. Chem.* **2012**, *84*, 8871–8879; c) B. Tang, N. Zhang, Z. Z. Chen, K. H. Xu, L. H. Zhuo, L. G. An, G. W. Yang, *Chem. Eur. J.* **2008**, *14*, 522–528.
- [21] a) X. Jiang, C. Röcker, M. Hafner, S. Brandholt, R. M. Dörlich, G. U. Nienhaus, *ACS Nano* **2010**, *4*, 6787–6797; b) L. Shang, G. U. Nienhaus, *Mater. Today* **2013**, *16*, 58–66.
- [22] a) H. B. Yu, Y. Xiao, L. J. Jin, *J. Am. Chem. Soc.* **2012**, *134*, 17486–17489; b) L. X. Yang, L. Shang, G. U. Nienhaus, *Nano-scale* **2013**, *5*, 1537–1543.

- [23] W. G. Kreyling, A. M. Abdelmonem, Z. Ali, F. Alves, M. Geiser, N. Haberl, R. Hartmann, S. Hirn, D. J. de Aberasturi, K. Kantner, G. Khadem-Saba, J. M. Montenegro, J. Rejman, T. Rojo, I. R. de Larramendi, R. Ufartes, A. Wenk, W. J. Parak, *Nat. Nanotechnol.* **2015**, *10*, 619–623.
- [24] L. Shang, S. Brandholt, F. Stockmar, V. Trouillet, M. Bruns, G. U. Nienhaus, *Small* **2012**, *8*, 661–665.
- [25] S. Kumar, W.-K. Rhim, D.-K. Lim, J.-M. Nam, *ACS Nano* **2013**, *7*, 2221–2230.
- [26] a) A. Meister, M. E. Anderson, *Annu. Rev. Biochem.* **1983**, *52*, 711–760; b) T. Jungas, I. Motta, F. Duffieux, P. Fanen, V. Stoven, D. M. Ojcius, *J. Biol. Chem.* **2002**, *277*, 27912–27918; c) B. Kim, G. Han, B. J. Toley, C. Kim, V. M. Rotello, N. S. Forbes, *Nat. Nanotechnol.* **2010**, *5*, 465–472.
- [27] a) M. Kim, S.-K. Ko, H. Kim, I. Shin, J. Tae, *Chem. Commun.* **2013**, *49*, 7959–7961; b) E. Ju, Z. Liu, Y. D. Du, Y. Tao, J. S. Ren, X. G. Qu, *ACS Nano* **2014**, *6*, 6014–6023.

Received: December 23, 2015

Revised: January 30, 2016

Published online: February 25, 2016